

RESEARCH ARTICLE | DECEMBER 02 2011

Impact of adsorbed organic monolayers on vacuum electron tunneling contributions to electrical resistance at an asperity contact

D. Berman; M. J. Walker; C. D. Nordquist; J. Krim



Journal of Applied Physics 110, 114307 (2011)

<https://doi.org/10.1063/1.3664770>



CrossMark

500 kHz or 8.5 GHz?
And all the ranges in between.

Lock-in Amplifiers for your periodic signal measurements



Find out more



Impact of adsorbed organic monolayers on vacuum electron tunneling contributions to electrical resistance at an asperity contact

D. Berman,^{1,a)} M. J. Walker,² C. D. Nordquist,³ and J. Krim¹

¹*Department of Physics, North Carolina State University, Raleigh, North Carolina 26795, USA*

²*Department of Materials Science and Engineering, North Carolina State University, Raleigh, North Carolina 26795, USA*

³*Sandia National Laboratories, Albuquerque, New Mexico 87185, USA*

(Received 25 August 2011; accepted 23 October 2011; published online 2 December 2011)

Electrical contact resistance measurements are reported for RF micro-electromechanical switches situated within an ultrahigh vacuum system equipped with *in situ* oxygen plasma cleaning capabilities. Measurements were performed on fused (permanently adhered) switches with Au/Au contacts and functioning switches with Au/RuO₂ contacts in both the presence and absence of adsorbed monolayers of pentane and dodecane. For switches adhered in the closed position, adsorption occurs only in regions external to direct contact. For functioning switches, however, it can occur either within or exterior to the contact. The data are analyzed within the framework of two distinct geometries, to explore how the presence of adsorbed molecules in regions close to the contact may impact vacuum tunneling contributions to the experimentally measured resistance: (1) The resistance associated with direct contact in parallel with a vacuum tunneling path, which upon uptake of the monolayer is replaced by the molecular resistance and (2) a series connection of the direct contact resistance with the molecular layer after adsorption occurs, with the vacuum tunneling path assumed to be negligible. In all cases, the experimental results quantitatively favor scenario (1), whereby uptake of the molecular layer effectively shuts down the vacuum tunneling path, in this case approximately 30 Ω in the absence of an adsorbed film. The methods described herein thus constitute a new and original approach to documenting vacuum tunneling levels in regions of close proximity. © 2011 American Institute of Physics. [doi:10.1063/1.3664770]

I. INTRODUCTION

The physics of electrical current flow through an asperity contact is a topic of wide-ranging impact, spanning tribological applications,^{1–4} to radio frequency microelectromechanical systems (RFMEMS) switches,^{5–8} to static charge transfer effects in materials of interest to the textiles industry.⁹ Surface roughness plays a key role in electrical current levels, since only the outermost asperities come into direct contact when two surfaces are brought into contact.^{10–12} For the case of RFMEMS switches,^{13–15} only a limited number of asperities come into contact, and only a few of the larger contacts are thought to carry most of the current.^{16–19} This characteristic allows RFMEMS switches to be conveniently approximated and modeled as single and/or few asperity contacts. It is well known that physisorbed layers condense onto gold surfaces²⁰ in both vacuum and ambient conditions, and that the coverage is determined by the pressure surrounding the surface^{21,22} and the uniformity of the substrate.^{23,24} At room temperature, the adsorbates are largely composed of hydrocarbon species and water vapor.^{21,24} Gold-on-gold (Au/Au) contacts are routinely employed experimentally to minimize the complicating effects of such layers, but the insulating films that remain on the contacts have a tremendous impact on their properties.^{13,25,26} It is moreover difficult to determine

whether the films are mostly situated within, or exterior to, regions of direct metal-metal contact. But if the films are removed, the switches become very susceptible to adhesive failure.

We focus here on vacuum electrical tunneling currents that may be present in regions^{27–31} that are in close proximity to regions of direct contact and the relative proportions of these compared to current flow through regions of direct contact. The results, which are motivated by measurements recently reported by Walker *et al.*,³² are of interest to communities far beyond RFMEMS, for example, in the areas of molecular electronics^{33,34} and carbon nanotube electrical contacts.^{35–38} Walker *et al.*³² performed measurements of dodecane gas uptake on gold-ruthenium oxide (Au/RuO₂) RFMEMS switches and observed the electrical contact resistance (ECR) to first double at sub-saturation pressures and then remain constant even for full monolayer coverages. The factor of two increase was unexpectedly small, because a dielectric material (for dodecane, $K = 2$) confined within a contact is expected to increase the resistance by many orders of magnitude.^{25,26,39} As a possible explanation, Walker *et al.* suggested that hydrocarbon molecules might be located just outside of the contact rather than within it.^{40–45} The resistance increase would then possibly be resulting from elimination of the tunneling currents present in vacuum for regions close to the contact.

In the work presented here, we seek to explore this hypothesis by systematically adsorbing molecules onto the

^{a)}Author to whom correspondence should be addressed. Electronic mail: dyanchu@ncsu.edu.

surfaces of RFMEMS switches while monitoring the change in resistance as a function of the surrounding gas pressure. We perform measurements on switches that are both operational and inoperational, i.e., adhered permanently in the closed position. In the latter case, adsorption occurs only in regions external to the directly contacting areas. The approach is depicted schematically in the lower portion of Figure 1. Adsorbed molecules in regions of near proximity to the direct contact are assumed to suppress or eliminate vacuum tunneling contributions, thus increasing the effective resistance of the contact. The total electric current at an asperity I is thus comprised of vacuum tunneling I_{tv} and direct contact I_c components, $I = I_{tv} + I_c$. Under this assumption, the experimentally measured contact resistance is lower than the direct contact resistance, $R < R_c$, since it is comprised of the parallel combination of R_c and R_{tv}

$$R_{parallel} = \frac{R_c * R_{tv}}{R_c + R_{tv}}. \quad (1)$$

The paper is divided into 6 sections. Section II describes the experimental setup and data taking procedure. ECR data are presented in Sec. III, for measurements of pentane uptake on clean Au/Au contacts adhered in the closed position, and for pentane uptake on functioning Au/RuO₂ contacts. Au/RuO₂ contacts have higher resistance, but approximately the same electron tunneling properties, since the electron work functions are close for gold (~5.3 eV), ruthenium (~4.7 eV), and ruthenium oxide (~5.1 eV). In Sec. III, we also present measurements performed with a longer chain molecule, namely dodecane. If the hypothesis is correct, the gases will produce similar results because both pentane and dodecane are large enough to suppress tunneling.

In Sec. IV, two models of hydrocarbon impact on switch resistance are examined: (1) the resistance associated with direct contact R_c is assumed to be in parallel with a vacuum tunneling path R_{tv} , which upon uptake of the monolayer is

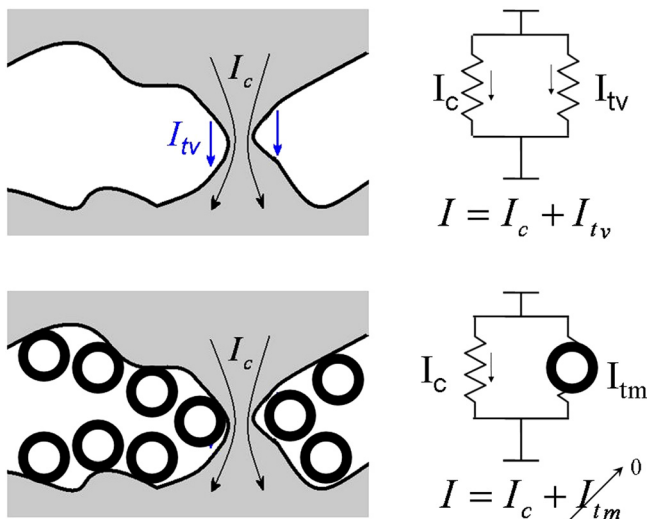


FIG. 1. (Color online) Schematic of our experimental approach for the ECR of an adhered switch. The current through regions of direct contact, I_c , adds to that associated with vacuum tunneling, I_{tv} . Adsorbed molecules suppress the vacuum tunneling component and replace it with I_{tm} , assumed negligible in this work.

replaced by the molecular resistance R_{tm} and (2) the molecular layer resistance R_{tm} (after adsorption within the contact) is assumed to form a series connection with the direct contact resistance, R_c , and vacuum tunneling mechanisms presumed to be negligible. In these models, we neglect the effects of tunneling material transfer, as this has not been reported to have a large impact on the magnitude of the resistance.⁴⁶ As will be reported, the experimental results all favor a scenario whereby uptake of the molecular layer effectively shuts down the vacuum tunneling path, which for the switches studied here has an effective resistance of ~30 Ω in advance of molecular uptake. Sections V and VI include discussion and concluding remarks.

II. EXPERIMENTAL PROCEDURE

Two different types of switches were employed for these studies, fabricated at either Radio Frequency MicroDevices (RFMD)⁴⁷ or Sandia National Lab (SNL). They have been described in detail in prior publications.^{48,49}

RFMD Au/Au switches were used for the permanent contact (fused switch) experiments.⁴⁸ The RFMD switch is an inline metal contacting switch. The transmission signal enters at the anchor or fixed end and travels the length of the cantilever beam and exits to the transmission line through the contacts at the end of the cantilever beam. Because the signal must travel through the cantilever beam, the cantilever is fabricated using a thick layer of electroplated gold (~10 μm). The contact resistance is approximately 1 Ω , and resistance of the wires with all connections was measured to be approximately 0.1 Ω , which is small compared to the resistance of the switches themselves. Rezvani *et al.*¹⁶ calculated a theoretical resistance of ~0.1 Ω for the switches under a 50 μN contact force, which is clearly lower than the experimentally measured value. Because the RFMD switches were initially open, a contamination layer is likely to be present at the fused contacts, thus explaining the difference with theory.

The Au/RuO₂ switches were fabricated, released, and wirebonded at SNL. Each die consists of 12 switches divided into three isolated banks of four. Each bank of four switches share two common ground pads, one sense pad and one source pad to enable four wire resistance measurements at the switch, itself. Each device has a dedicated actuation pad to close specific switches. Each ground pad is wirebonded to the package bottom to mitigate electrostatic discharge. All top contacts are gold, while the bottom contacts are either reactively sputtered RuO₂ or sputtered Ru that is oxidized after deposition, as described in detail in an earlier publication.⁴⁹ The actuation voltage to close SNL switches range from 87 to 99 V, corresponding to 280 to 365 μN .^{50,51} Since the oxygen plasma cleaning process causes the two substrate materials to become similar,^{49,52-54} they were not distinguished in these studies.

The MEMS stage at North Carolina State University consists of two custom built rectangular machinable glass ceramic pieces with an array of holes drilled out to support 24, 40, and 64 pin packages. These ceramic pieces are suspended inside an ultra high vacuum (UHV) chamber. All pin sockets connect to standard vacuum wires by spot welding, to

reduce the possibility of outgassing in vacuum and during plasma cleaning. Two Cu discs are mounted on both sides of the MEMS stage and connect to a high voltage power supply for generating *in-situ* plasma.^{32,49} A quartz crystal microbalance (QCM) with polished gold electrodes is positioned in close proximity to gauge adsorbate uptake levels on the switch contact pads. When gases adsorb onto both sides of an AT-cut QCM, the change in frequency can be calculated by⁵⁵

$$\delta f = \frac{4f^2\sigma}{\rho_q v_q}, \quad (2)$$

where f is the frequency of the QCM $f=8$ MHz, σ is the areal density of the adsorbate in g/cm^2 , $\rho_q=2.648$ g/cm^3 is the density of quartz, and $v_q=3.338 \times 10^5$ cm/s is the speed of sound in quartz. The measured drift of the QCM was 0.1 Hz/h or less, and all of the measurements were recorded in less than 15 min.

We did not observe argon plasma (120 mTorr of Argon for 300 s) to be effective in cleaning the switches. We did, however, observe that oxygen plasma exposure reduced the contact resistance of both Au and Ru based switches to values lower than obtained by operating the switches in UHV alone and that oxygen plasma exposure times longer than about 5 min did not result in further lowering of the resistance. The contact resistance of switches operated or simply left open in vacuum was always observed to increase, but subsequent exposure to oxygen plasma allowed the contact resistance to be returned to its original values. This reproducible contact resistance after oxygen plasma exposure served as the baseline for the experiments reported here. We have also observed that oxygen plasma induced thickening of oxide layers on the bulk sample causes the two samples to have very similar properties.^{49,52–54}

Oxygen plasma cleaning treatments were performed as follows: all actuation voltage and four wire resistance connections outside the chamber were disconnected from the feedthroughs and a gate valve connecting the sample chamber to the ion pump was closed. Research grade O_2 was then leaked into the sample chamber until a capacitance manometer pressure gauge read approximately 150 mTorr. The system was then pumped with a turbo molecular pump, connected through a regulating valve adjusted to maintain a pressure of 150 mTorr. One Cu disc was next connected to a potential of 0.4 kV, while the other Cu disc was connected to both the grounded vacuum chamber and the ground of the power supply. Switches were exposed to oxygen plasma for 5 min, and then the power supply was turned off and the chamber pumped immediately to 10^{-8} Torr with the turbomolecular pump followed by the ion pump.

III. DATA COLLECTION AND RESULTS

A. Measurement #1: Pentane adsorption on a permanently closed Au/Au switch

As an initial experiment, to probe uptake in a situation where gas uptake is limited to regions external to the contact, we examined RFMD Au/Au switches that were adhered in the closed position. For this experiment, no actuation

voltage, and thus no external load, was applied to the contact. The switches provided a convenient means to perform the experiments with the same parameters and in the same environments as for working switches. In addition, the contact resistance is time independent for adhered switches, simplifying the data analysis.⁴⁸

Experimental resistance values R were measured both before and after oxygen plasma cleaning using a four probe resistance technique, with a voltage source of 0.02 V. In the absence of a cleaning treatment, exposure to pentane vapors caused no changes in R .

This result is consistent with our hypothesis that adsorbed contaminants largely suppress tunneling currents in regions surrounding the direct contact.

After 40 s of oxygen plasma cleaning, 3 of the switches exhibited reductions in resistance consistent with cleaning of residual contaminants, and after 300 s, all 6 of the switches studied displayed such behavior. The resistance of the cleaned switches moreover became sensitive to the presence of pentane gas vapors, as depicted in Figure 2, which shows resistance versus pentane pressure data for the two groups of switches, whereby exposure to pentane vapor at 10^{-3} Torr

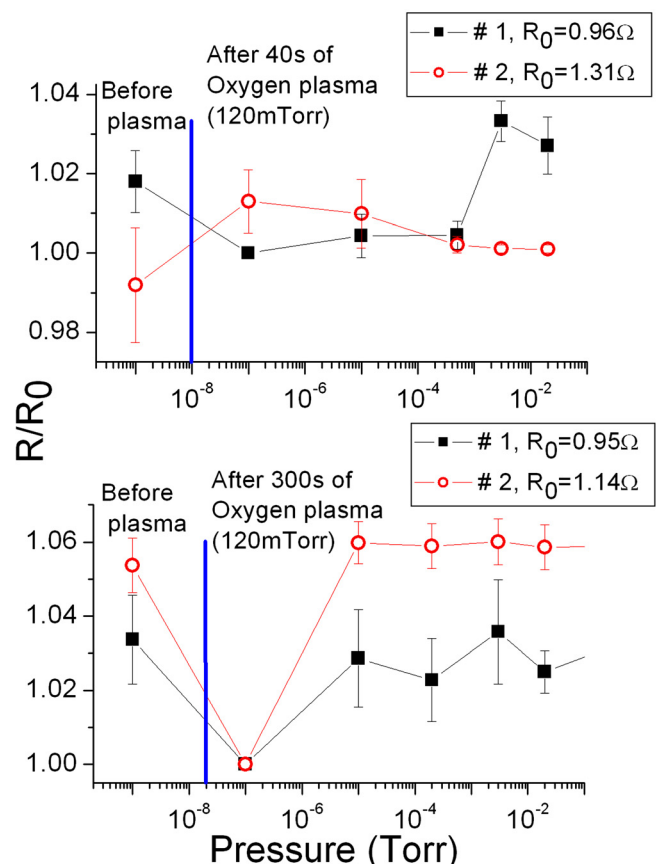


FIG. 2. (Color online) Experimentally measured total switch resistance R divided by its value immediately after plasma cleaning R_0 , at 10^{-7} Torr, versus surrounding pentane pressure for two groups of fused Au/Au switches. The switches were cleaned for 300 s after recording the data set in the upper portion of the figure. Each group consists of three different switches and average resistance of the switches is presented by black filled squares and empty red circles accordingly. Results are presented for 40 s and 300 s plasma cleaning procedure. The bulk vapor pressure of pentane at room temperature is 419 Torr. QCM uptake data for pentane/Au are displayed in the inset to Figure 3.

(40 s) and 10^{-7} Torr (300 s) levels caused the resistance values to increase back to their original, pre-cleaned levels. The lower uptake pressure after 300 s of cleaning is presumed to be associated with the increased surface roughness that results from the cleaning procedure.

Equation (1), the parallel combination resistance of R_c in parallel with R_{tv} provides a means to estimate the relative tunneling and direct contact contributions: The resistance in vacuum (1Ω) is assumed to be $R_{parallel}$, while the resistance in the presence of adsorbed pentane ($1.04 \pm 0.01 \Omega$) is assumed to be R_c (Figure 1). Substituting these values into Eq. (1) yields a value of $\sim 26 \Omega$ for the effective resistance associated with vacuum tunneling mechanisms,

$$R_{tv} = \frac{R_c * R_{parallel}}{R_c - R_{parallel}} = \frac{1.04 * 1}{1.04 - 1} = \frac{1.04}{0.04} = 26 \Omega. \quad (3)$$

In the experiments described next, we repeat the measurements on switches that have similar tunneling properties but larger R_c . According to Eq. (1), an adsorbed gas should have greater influence in this case, since it eliminates a larger proportion of the total current flow.

B. Measurement #2: Pentane adsorption on operational Au/RuO₂ switches

Tunneling current depends on the work function of both the tip and the substrate, which are close for gold, ruthenium, and ruthenium oxide (a detailed calculation is presented in Sec. IV). Therefore, to further explore the previous suggestion that pentane uptake results in suppression of vacuum tunneling contributions, the gold-on-gold switches were replaced with gold/ruthenium switches, a materials combination that exhibits a higher experimentally measured contact resistance R_c (10–15 Ω). This material combination also exhibits an excellent response to oxygen plasma cleaning.⁴⁹ All experiments were performed with working switches, because clean Au/RuO₂ contacts do not permanently adhere in the closed position. They are thus excellent candidates for commercial applications.

Figure 3 shows switch resistance values versus surrounding pentane pressure for oxygen plasma cleaned Au/RuO₂ switches. The switches were cleaned for 300 s before data taking commenced. The actuation voltage to close the switches ranged from 87 to 99 V, corresponding to 280 to 365 μN .^{50,51} Once a device was closed, the actuation voltage was held constant for over 30 min to allow the time dependence of the contact resistance to be documented. The switch was then reopened and exposed to a higher pentane pressure. Pentane exposure caused the switch resistance to increase by a factor of 2, a much larger factor than observed for the Au/Au switches. The switch resistance doubles for devices at pressures near 10^{-2} Torr and fails to increase significantly thereafter. This shape is similar to that reported by Koidl *et al.* for “critical concentration” adsorption uptakes^{56,57} on macroscopic switches, whose initial resistances fell in the range 0.005–0.007 Ω .

Koidl *et al.* recorded measurements of switch resistance in a synthetic air (80% nitrogen, 20% oxygen) and defined the critical concentration level as the point where switch

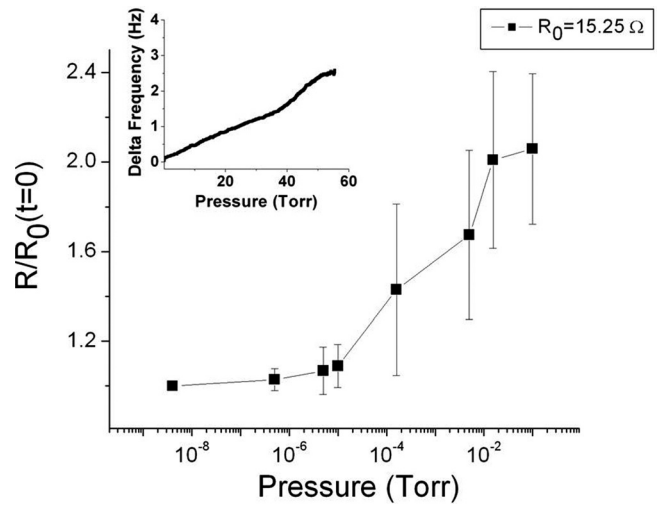
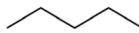
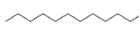


FIG. 3. Initial switch resistance (R is the resistance measured upon first time closure at $t=0$) divided by its initial value after cleaning (R_0 is the resistance of the switches after plasma cleaning at $t=0$) versus surrounding pentane pressure. The switch resistance doubles for devices at pressures of 10^{-2} Torr. They fail to increase significantly thereafter, even for full monolayer coverages of pentane. The inset represents frequency shift versus pentane pressure for a quartz crystal microbalance with gold electrodes situated near the RFMEMS switches. The bulk vapor pressure at room temperature is 419 Torr (Ref. 58), and one monolayer of pentane adsorbed on the electrodes corresponds to a 3.8 Hz shift.

resistance exceeded 0.1 Ω . They suggested that an oxygen deficient environment should lower the critical concentration by more than 2 orders of magnitude. They interpreted this as a protective property of oxygen, given that carbon deposits in an oxygen deficient environment are inhibited from forming a volatile oxide. Critical concentrations by this argument are then expected to be extremely low in vacuum environments, since perfect vacuum is completely depleted of oxygen. From this perspective, our observation of an abrupt increase in resistance at a very low partial pressure of pentane in vacuum is entirely consistent with the prior reports. Table I tabulates the critical concentrations for both the work of Koidl *et al.* and Figure 3 values for pentane adsorption.

TABLE I. Summarizing pentane and dodecane values at critical concentrations and coverage at which the initial resistance increases by a factor of two. It is interesting that Koidl^{56,57} also observes a difference in critical concentration in a synthetic air but only about 30 \times instead of 1000 \times .

	This work	Pentane	Dodecane
			
Critical concentration (Torr)		0.05–0.1	5×10^{-5}
Partial pressure		2.39×10^{-4}	1.25×10^{-4}
Area density (ng/cm ²)		32.7	32.6
Coverage of a monolayer		1.3×10^{-2}	2.6×10^{-3}
	Koidl	Pentane	Dodecane
Critical concentration (Torr)		>7.6	0.266
Partial pressure		0.0185	0.887
Area density (ng/cm ²)		NA	NA
Coverage of a monolayer		NA	NA
Vapor pressure at RT (Torr)		418.62 (Ref. 58)	0.3 (Ref. 60)

Equation (1), the parallel combination resistance of R_c with R_{tv} , provides a means to estimate the proportions of tunneling to direct contact contributions: The resistance in vacuum (15 Ω) is assumed to be $R_{parallel}$, while the resistance in the presence of adsorbed pentane ($\sim 30 \Omega$) is assumed to be R_c (Figure 1). Substituting these values into Eq. (1) yields a value of 30 Ω for the effective resistance associated with vacuum tunneling mechanisms,

$$R_{tv} = \frac{R_c * R_{parallel}}{R_c - R_{parallel}} = \frac{30 * 15}{30 - 15} = \frac{300}{15} = 20 \Omega. \quad (4)$$

The inset to Figure 3 depicts the frequency shift of the QCM as pentane is leaked into a chamber initially at 10^{-9} Torr. The mass per unit area of an adsorbed pentane ($\text{CH}_3(\text{CH}_2)_3\text{CH}_3$) monolayer is well documented for the case of uptake on a gold surface.⁵⁹ For molecules oriented with the hydrocarbon backbones parallel to the surface, each molecule (1.2×10^{-22} g or molecular weight 72.15) can be assumed to occupy a 36.6×10^{-22} nm² rectangular area on the surface, corresponding to $\sigma = 32.7$ ng/cm². For a 5 MHz resonant frequency QCM, this corresponds to a 3.78 Hz frequency shift per monolayer (from Eq. (2)). Clearly this is an estimate, as only one of the contacts is gold, and the geometry is far from planar, but the information is nonetheless useful to document that uptake is indeed occurring. We also note that the resistance changes begin at pressures lower than where QCM first begins to detect uptake. The best explanation for this is the fact that the binding energy for adsorption close to the contact is expected to be substantially greater than that of the open geometry of the QCM electrode: in short, the adsorbed particles close to the switch contact are coming into contact with multiple surfaces. The QCM measurements of coverage remain relevant, however, as an important reference point for comparison purposes.²³

The tunneling resistance of 30 Ω obtained in the second experiment is very close in magnitude to the 26 Ω observed for the Au/Au contacts, lending support for the hypothesis that vacuum tunneling is contributing at this level. To further explore this hypothesis, we adsorbed dodecane gas rather than pentane. If our hypothesis is correct, then the resistance increase will be comparable for the two gases, since both are expected to suppress the tunneling current even though dodecane is a longer chain molecule.

C. Measurement #3: Dodecane adsorption on operational Au/ RuO₂ switches

Figure 4 shows normalized switch resistances (for the same switches utilized in measurement #2) as dodecane is leaked into the sample cell. The resistance increases by the factor of 2 in a manner similar to pentane, but at a much lower pressure: 5×10^{-5} Torr. The resistance then levels off after 5×10^{-4} Torr. This shape is similar to what Koidl *et al.*^{56,57} reported for their critical concentration adsorption uptakes. Table I tabulates the critical concentrations for both the works by Koidl *et al.* The critical concentration in the work of Koidl *et al.* is 0.266 Torr, but for this work, the critical concentration is $\sim 5 \times 10^{-5}$ Torr. Again, this may also be

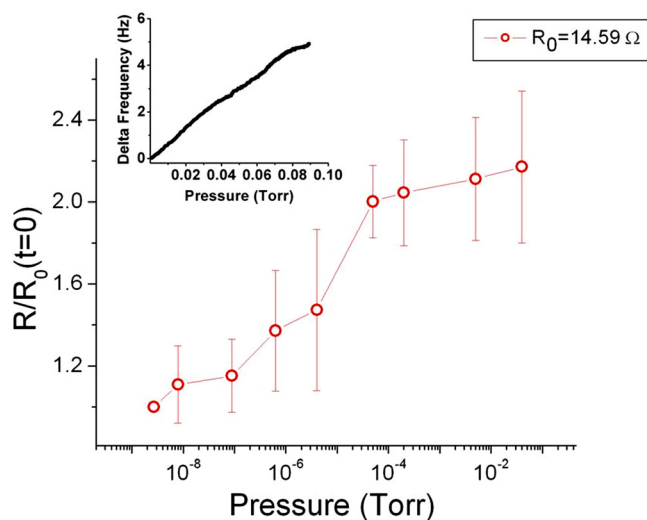


FIG. 4. (Color online) Initial switch resistance (R is the resistance measured upon first time closure at $t=0$) divided by its initial value after cleaning (R_0 is the resistance of the switches after plasma cleaning at $t=0$) versus surrounding dodecane pressure. The switch resistance doubles for devices at pressures of 10^{-5} Torr. It fails to increase significantly thereafter, even for full monolayer coverages of dodecane. The inset depicts frequency shift versus dodecane pressure for a quartz crystal microbalance with gold electrodes situated near the RFMEMS switches. The bulk vapor pressure of dodecane at room temperature is 0.3 Torr (Ref. 60), and one monolayer of dodecane adsorbed on the electrodes corresponds to a 3.8 Hz shift.

related to either the plasma-induced surface roughness or the fact that the macroscopic switches have larger contact pressures, so the adsorbates are more readily squeezed out of the contact.

The inset to Figure 4 is the frequency shift of a QCM as dodecane is leaked into a chamber whose base pressure was initially at 10^{-9} Torr. The mass per unit area of an adsorbed dodecane ($\text{CH}_3(\text{CH}_2)_{10}\text{CH}_3$) monolayer is well documented for the case of uptake on a gold surface.⁶¹ For molecules oriented with their hydrocarbon backbones parallel to the surface, each molecule (2.839×10^{-22} g or molecular weight 170) can be assumed to occupy a $1.73 \text{ nm} \times 0.5 \text{ nm}$ rectangular area on the surface, corresponding to $\sigma = 32.6$ ng/cm². For a 5 MHz resonant frequency QCM, this corresponds to a 3.78 Hz frequency shift per monolayer.

Figure 5 presents pentane and dodecane data from Figures 3 and 4 on the same plot, but plotting them as a function of P/P_0 rather than P , where P_0 is the bulk saturation pressure. The resistance increase occurs at almost the same partial pressures for pentane and dodecane and the increases are within experimental error of each other.

IV. PARALLEL AND SERIES MODELS OF MOLECULAR ADSORPTION ON SWITCH RESISTANCE

We now consider two theoretical models, a parallel connection model and a series connection model, to explore the physical nature of the increase in resistance that occurs upon molecular uptake. Since the resistance change is completely reversible, we have documented that uptake and removal of the molecules is causing the change. We now consider which physical location for the molecules is most likely resulting in the resistance change.

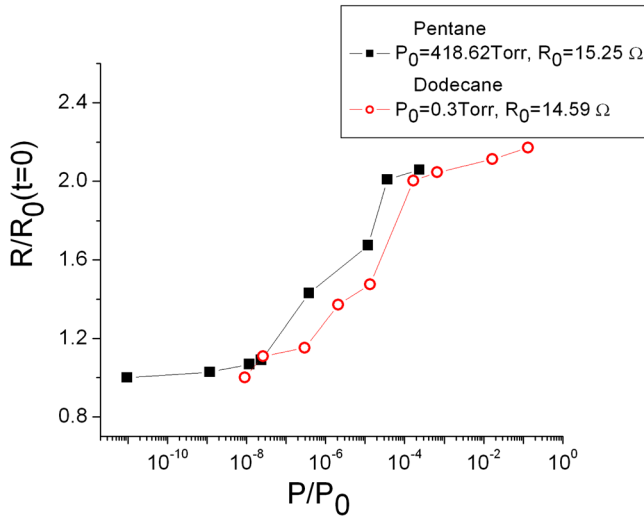


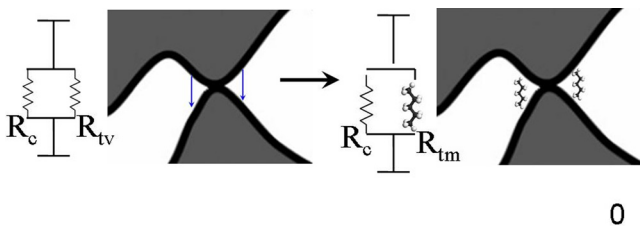
FIG. 5. (Color online) Relative switch resistance versus partial pressure of pentane (black filled squares) and dodecane (red empty circles). The resistance approximately doubles in both cases for partial pressures of 10^{-4} . P_0 is the bulk vapor pressure.

A. Parallel connection

The total switch resistance in the parallel connection model, $R_{parallel}$, is determined from the sum of the reciprocals of contact resistance R_c and effective tunneling current resistance in vacuum R_{tv} (Eq. (1)). Hydrocarbon molecules adsorbed on the surface contribute tunneling resistance through molecules R_{tm} , which is assumed to be much larger than R_{tv} , thus suppressing the tunneling current and increasing the total switch resistance $R_{parallel}$ so that it is effectively equal to R_c (Figure 6). Simmons³⁹ obtained the tunneling current density j_t for electrons tunneling through a potential barrier φ (reflective of the combined tip/substrate work functions) of thickness Δz ,

$$j_t = \frac{e}{2\pi h(\Delta z)^2} \left[\varphi e^{-4\pi\sqrt{\frac{2m\varphi}{\hbar^2}}\Delta z} - (\varphi + eV)e^{-4\pi\sqrt{\frac{2m(\varphi+eV)}{\hbar^2}}\Delta z} \right], \quad (5)$$

where V is potential difference between tip and substrate in Volts ($V=0.02$ V in measurements presented here), $e=1.6 \times 10^{-19}$ C and $m=9.1 \times 10^{-31}$ kg are the charge in Coulombs and the mass in kilograms of the electron,



$$\frac{1}{R} = \frac{1}{R_c} + \frac{1}{R_{tv}} \quad \longrightarrow \quad \frac{1}{R} = \frac{1}{R_c} + \frac{1}{R_{tm}}$$

FIG. 6. (Color online) Contact resistance R_c and effective tunneling resistance R_{tv} in A parallel connection. Adsorbed hydrocarbon molecules are assumed to suppress the tunneling current, and the tunneling current through the molecule is assumed to be negligible.

respectively, $h=6.6 \times 10^{-34}$ Js is the Planck constant, φ is average barrier height, in Joules, relative to the Fermi level of the negative electrode. As a simplification, φ is taken as the average of gold and ruthenium oxide work functions, or ~ 5 eV. If $\varphi \gg Ve$ (as in the present experimental case, with $V=0.02$ V, 5 eV $\gg 0.02$ eV), then Eq. (5) can be simplified to

$$j_t = \frac{e^2 k V}{4\pi h \Delta z} \exp(-k \Delta z), \quad (6)$$

where

$$k = \frac{4\pi\sqrt{2m\varphi}}{h}. \quad (7)$$

Employing the values of $\varphi=5$ eV $= 8 \times 10^{-19}$ J, $e=1.6 \times 10^{-19}$ C, $m=9.1 \times 10^{-31}$ kg, and $H=6.6 \times 10^{-34}$ Js, the value of coefficient k is

$$K = 2.3 \times 10^{10} \text{m}^{-1}. \quad (8)$$

The effective tunneling resistance can be estimated as

$$R_{tv} = \frac{V}{I_t} = \frac{V}{j_t S} = \frac{4\pi h \Delta z}{e^2 k \exp(-k \Delta z) S_t}, \quad (9)$$

$$\begin{aligned} R_{tv} &= \frac{4 * 3.14 * 6.6 * 10^{-34} * \Delta z}{(1.6 * 10^{-19})^2 * 2.3 * 10^{10} * \exp(-2.3 * 10^{10} * \Delta z) * S_t} \\ &= 1.4 * 10^{-5} * \frac{\Delta z}{\exp(-k \Delta z) S_t}, \end{aligned} \quad (10)$$

where S_t is the effective tunneling area. We now estimate the value of S_t .

Rezvanian *et al.*¹⁶ reported that the average number of asperities N in contact after 30 min is about 40, and the average size of a contact area radius r is 40 nm.⁶² To estimate the effective tunneling area, we assume that current flows at up to 1 gold atom in lateral extent around the contacts. Because the tunneling current density value decreases by orders of magnitude with changing the distance by even as little as 1 Å, the effect from tunneling current through surrounding areas that are further away is neglected. The effective tunneling area S_t , approximated by a one-atom wide annulus defined by the perimeter of the asperities multiplied by the number of asperities, therefore, is found (for a gold atomic radius $r_{Au}=144 \times 10^{-12}$ m) to be

$$S_t = P * r_{Au} * N = 2 * \pi * r * r_{Au} * N \approx 1.5 * 10^{-15} \text{m}^2. \quad (11)$$

If $\Delta z=1.44 \times 10^{-10}$ m (the gold atomic radius), then

$$\begin{aligned} S_t R_{tv} &= (1.5 * 10^{-15} \text{m}^2)(37 \Omega) = 5.55 * 10^{-14} \Omega \text{m}^2; \\ R_{tv} &= 37 \Omega \end{aligned} \quad (12)$$

We emphasize that the value of 37 Ω for the tunneling resistance is an estimate and the actual R_{tv} may vary, depending on the actual value of S_t .

Adding hydrocarbons to the switch environment results in surface contamination around the contacts and converts the tunneling resistance in vacuum R_{tv} into the tunneling resistance through the molecules R_{tm} . The effective tunneling resistance of hydrocarbons R_{tm} (100–10000 Ω) is assumed to be much larger than the direct contact resistance R_c , and so effectively suppresses the tunneling current. The total resistance $R_{parallel}$ of the switches with adsorbed hydrocarbons present is therefore essentially the contact resistance R_c itself. A quantitative estimate of R_{tm} depends on whether or not the molecules are treated as individual resistors, as in the field of molecular electronics. In this case, Eq. (5) is difficult to apply, as the molecular orientation is convoluted with its resistance. This is discussed in Sec. IV B.

If for plasma cleaned Au/RuO₂ switches, the contact resistance and tunneling current resistance work in parallel, producing the total resistance of 15 Ω , then the resistance of Au/RuO₂ contacts is evaluated to be 30 Ω . If the contact resistance of fused gold-on-gold switches is ~ 1 Ω , then the tunneling current impact on switch resistance is only 3%-5%.

This model thus explains all of the measurements we have recorded. The resistance of the contacts is also not expected to be impacted by further uptake of hydrocarbons because the contact force is high enough to push hydrocarbon molecules aside.⁶³

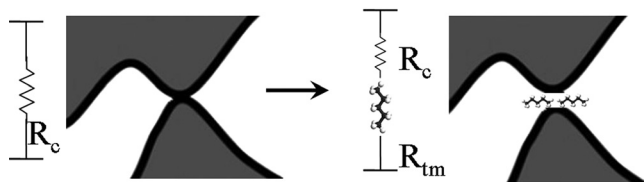
We now explore whether a series connection is also able to explain the experimental results.

B. Series connection

In our second model, we assume that hydrocarbon molecules form a layer between the contacts, which results in an increase in switch resistance denoted by R_{series} , the sum of the resistance of the adsorbed layer in series R_{tm} to the contact resistance R_c (Figure 7). The total area of the contact spots S_c is calculated by taking into account the average number of the asperities in the contact $N=40$, and the average asperity radius $r=40$ nm^{16,62}

$$S_c = N * (\pi * r^2) = 2 * 10^{-13} m^2. \quad (13)$$

We note that S_c is roughly 100 times greater than the tunneling area S_t calculated in the previous model, suggesting that the resistance of the hydrocarbons in the tunneling gap would need to be on the order of 100–10000 Ω for equivalent conduction contributions.



$$R_{series} = R_c \quad \longrightarrow \quad R_{series} = R_c + R_{tm}$$

FIG. 7. Contact resistance R_c and resistance of hydrocarbon molecules R_{tm} in series connection.

The surface area of pentane molecules is $S_{pentane} = 36.6 \times 10^{-2} \text{ nm}^2$ (Ref. 55) and the approximate number of molecules on the surface is

$$N_{molecules} = \frac{S_c}{S_{pentane}} \approx 10^6. \quad (14)$$

Paulsson *et al.*⁶⁴ reported the resistance of organic molecules to be on the order of 10^6 – 10^8 Ω . Therefore, the molecules (as 10^6 resistors in parallel) can potentially act as a ~ 1 – 100 Ω resistor, which does encompass the value of the additional resistance observed for the Au/RuO₂ switches, whose values increased by 15 Ω . However, there are several inconsistencies between the series conduction model and the measured results:

1. The resistance of the layer should be extremely sensitive to its thickness, an effect that we do not observe.
2. Wold and Frisbie⁶³ reported that 100 nN contact forces were sufficient to displace self-assembled monolayers (SAM) from Au/Au contacts in an atomic force microscopy (AFM) geometry. Patton *et al.*¹⁵ later reported SAM displacement for Au/Au MEMS contacts under 200 μN contact forces. In experiments presented in this paper, the contact force of ~ 300 μN (Refs. 50 and 51) is used to actuate the switches. Hydrocarbon molecules are therefore very likely to have been pushed out of the contacts.
3. No resistance change would be predicted for the fused Au/Au contacts, contrary to what is observed.

V. SUMMARY AND CONCLUSIONS

We have performed electrical contact resistance measurements for RF micro-electromechanical switches situated within an ultrahigh vacuum system equipped with *in situ* oxygen plasma cleaning capabilities. Measurements were performed on fused (permanently adhered) switches with Au/Au contacts, and functioning switches with Au/RuO₂ contacts in both the presence and absence of adsorbed monolayers of pentane and dodecane. Measurements were performed after *in situ* oxygen plasma cleaning to remove residual surface contaminants. Our primary observations were

- (1) fused Au/Au switch resistances increased by 3%–5% (which corresponds to ~ 26 Ω tunneling resistance in parallel) after adding pentane to the switch environment.
- (2) Au/RuO₂ switch resistances approximately doubled for either pentane or dodecane uptake but exhibited the same tunneling resistance if a parallel connection is assumed (~ 30 Ω). Future work will investigate hydrocarbons effect on Au/RuO₂ switches in adhered position (which is difficult to achieve).
- (3) The data were analyzed within the framework of two distinct geometries: (1) The resistance associated with direct contact in parallel with a vacuum tunneling path, which upon uptake of the monolayer is replaced by the molecular resistance and (2) a series connection of the direct contact resistance with the molecular layer after adsorption occurs, with the vacuum tunneling path assumed to be negligible. In all cases, the experimental results quantitatively favor scenario (1).

- (4) The methods described here constitute a new and original approach to documenting vacuum tunneling levels in regions of close proximity. Future studies will focus on an investigation of the role of molecules in low contact pressure conditions to explore the series connection effects. Measurements on Au-RuO₂ contacts held permanently in a closed position would also be of interest.

ACKNOWLEDGMENTS

This work has been supported by NSF DMR0805204, the Extreme Friction MURI program, AFOSR # FA9550-04-1-0381, and the DARPA S&T Fundamentals Program, "Center for RF MEMS Reliability and Design Fundamentals," Grant No. HR0011-06-1-0051. Sandia National Laboratories is a multi program laboratory managed and operated by Sandia Corporation, a wholly owned subsidiary of Lockheed Martin Corporation, for the U.S. Department of Energy's National Nuclear Security Administration under contract DE-AC04-94AL85000. The authors acknowledge G. A. Patrizi, F. A. Austin, and Sandia MESAfab operations for switch fabrication and G. M. Rebeiz for visionary direction of the DARPA S&T program. Useful discussions with D. Dougherty, K. Komvopoulos, M. Zikry, D. A. Czaplewski, W. D. Cowan, and C. W. Dyck are greatly appreciated.

- ¹S. T. Patton and J. S. Zabinski, *Tribol. Lett.* **18**, 215 (2005).
²M. Belin, *Wear* **168**, 7 (1993).
³S. Hannel, S. Fouvry, P. Kapsa, and L. Vincent, *Wear* **249**, 761 (2001).
⁴C. Gao, D. Kuhlmannwilsdorf, and D. D. Makel, *Wear* **162**, 1139 (1993).
⁵J. W. Tringe, T. A. Uhlman, A. C. Oliver, and J. E. Houston, *J. Appl. Phys.* **93**, 4661 (2003).
⁶H. Kwon, S. S. Jang, Y. H. Park, T. S. Kim, Y. D. Kim, H. J. Nam, and Y. C. Joo, *J. Micromech. Microeng.* **18**, 105010 (2008).
⁷G. M. Rebeiz, *RF MEMS Theory, Design, and Technology* (Wiley, London, 2003).
⁸J. J. Yao, *J. Micromech. Microeng.* **10**, R9 (2000).
⁹J. V. Wasem, B. L. LaMarche, S. C. Langford, and J. T. Dickinson, *J. Appl. Phys.* **93**, 2202 (2003).
¹⁰B. Borovsky, J. Krim, S. A. Syed Asif, and K. J. Wahl, *J. Appl. Phys.* **90**, 6391 (2001).
¹¹J. A. Greenwood and J. B. P. Williamson, *Proc. R. Soc. London* **295**, 257 (1966).
¹²F. P. Bowden and D. Tabor, *Proc. Roy. Soc. London, Ser. A*, **169**, 391 (1939).
¹³D. J. Dickrell and M. T. Dugger, "The effects of surface contamination on resistance degradation of hot-switched low-force MEMS electrical contacts," in *Electrical Contacts Proceedings of the Fifty-First IEEE Holm Conference*, Chicago, IL, (2005), p. 255.
¹⁴R. Holm, *Electric Contact*, 4th ed. (Springer-Verlag, Berlin, 1967).
¹⁵S. T. Patton, K. C. Eapen, J. S. Zabinski, J. H. Sanders, and A. A. Voevodin, *J. Appl. Phys.* **102**, 024903 (2007).
¹⁶O. Rezvanian, M. A. Zikry, C. Brown, and J. Krim, *J. Micromech. Microeng.* **17**, 2006 (2007).
¹⁷D. G. Bansal and J. L. Streater, *Acta Mater.* **59**, 726 (2011).
¹⁸O. Rezvanian, C. Brown, M. A. Zikry, A. I. Kingon, J. Krim, D. L. Irving, and D. W. Brenner, *J. Appl. Phys.* **104**, 024513 (2008).
¹⁹C. Brown, O. Rezvanian, M. A. Zikry, and J. Krim, *J. Micromech. Microeng.* **19**, 025006 (2009).
²⁰J. Krim, J. G. Dash, and J. Suzanne, *Phys. Rev. Lett.* **52**, 640 (1984).
²¹V. Panella, R. Chiarello, and J. Krim, *Phys. Rev. Lett.* **76**, 3606 (1996).
²²K. R. Mecke and J. Krim, *Phys. Rev. B* **53**, 2073 (1996).
²³V. Panella and J. Krim, *Phys. Rev. E* **49**, 4179 (1994).
²⁴C. Mak and J. Krim, *Faraday Discuss.* **107**, 389 (1997).
²⁵L. Kogut and K. Komvopoulos, *J. Appl. Phys.* **95**, 576 (2004).
²⁶L. Kogut and K. Komvopoulos, *J. Appl. Phys.* **97**, 073701 (2005).
²⁷C. Li, E. T. Thostenson, and T.-W. Chou, *Appl. Phys. Lett.* **91**, 223114 (2007).
²⁸S. Xu, O. Rezvanian, K. Petters, and M. A. Zickry "Tunneling effects and electrical conductivity of CNT polymer composites," *MRS Proceedings*, 1304 (2011).
²⁹J. M. Pitarke, F. Flores, and P. M. Echenique, *Surf. Sci.* **234**, 1 (1990).
³⁰Y. A. Hong, J. R. Hahn, and H. Kang, *J. Chem. Phys.* **108**, 4367 (1998).
³¹B. Xu and N. J. Tao, *Science* **301**, 1221 (2003).
³²M. Walker, D. Berman, C. Nordquist, and J. Krim, *Tribol. Lett.* **44**, 305 (2011).
³³J. Y. Park, G. H. Kim, K. W. Chung, and J. U. Bu, *Sens. Actuators, A* **89**, 88 (2001).
³⁴H. W. C. Postma, T. Teepen, Z. Yao, M. Grifoni, and C. Dekker, *Science* **293**, 76 (2001).
³⁵Z. C. Wu, Z. H. Chen, X. Du, J. M. Logan, J. Sippel, M. Nikolou, K. Kamaras, J. R. Reynolds, D. B. Tanner, A. F. Hebard, and A. G. Rinzier, *Science* **305**, 1273 (2004).
³⁶H. J. Dai, E. W. Wong, and C. M. Lieber, *Science* **272**, 523 (1996).
³⁷T. W. Tomblar, C. W. Zhou, L. Alexseyev, J. Kong, H. J. Dai, L. Lei, C. S. Jayanthi, M. J. Tang, and S. Y. Wu, *Nature* **405**, 769 (2000).
³⁸B. Q. Wei, R. Vajtai, and P. M. Ajayan, *Appl. Phys. Lett.* **79**, 1172 (2001).
³⁹J. G. Simmons, *J. Appl. Phys.* **34**, 1793 (1963).
⁴⁰X. Bouju, Ch. Girard, H. Tang, C. Joachin, and L. Pizzagalli, *Phys. Rev. B* **55**, 16498 (1997).
⁴¹U. Kurpick and T. S. Rahman, *Phys. Rev. Lett.* **83**, 2765 (1999).
⁴²Y. H. Jang and J. R. Barber, *J. Appl. Phys.* **94**, 7215 (2003).
⁴³C. D. Lorenz, M. Chandross, and G. S. Grest, *J. Adhes. Sci. Technol.* **24**, 2453 (2010).
⁴⁴M. Abdelmaksoud, S. M. Lee, C. W. Padgett, D. W. Irving, D. W. Brenner, and J. Krim, *Langmuir* **22**, 9606 (2006).
⁴⁵D. W. Brenner, D. L. Irving, A. I. Kingon, and J. Krim, *Langmuir* **23**, 9253 (2007).
⁴⁶M. Vincent, S. W. Rowe, C. Poulain, D. Mariolle, L. Chiesi, F. Houze, and J. Delamare, *Appl. Phys. Lett.* **97**, 263503 (2010).
⁴⁷See <http://www.RFMD.com> for RF Micro Devices.
⁴⁸D. Berman, M. Walker, and J. Krim, *J. Appl. Phys.* **108**, 044307 (2010).
⁴⁹M. Walker, C. Nordquist, D. Czaplewski, G. Patrizi, N. McGruer, and J. Krim, *J. Appl. Phys.* **107**, 084509 (2010).
⁵⁰C. Brown, A. S. Morris, A. I. Kingon, and J. Krim, *J. Microelectromech. Syst.* **17**, 1460 (2008).
⁵¹V. V. Konchits and C. K. Kim, *Wear* **232**, 31 (1999).
⁵²Y. Iwasaki, A. Izumi, H. Tsurumaki, A. Namki, H. Oizumi, and I. Nishiyama, *Appl. Surf. Sci.* **253**, 8699 (2007).
⁵³I. Nishiyama, H. Oizumi, and K. Motai, *J. Vac. Sci. Technol. B* **23**, 3129 (2005).
⁵⁴Y. Abe, Y. Kaga, M. Kawamura, and K. Sasaki, *J. Vac. Sci. Technol. B* **18**, 1328 (2000).
⁵⁵G. Sauerbrey, "Verwendung von Schwingquarzen zur Wägung dünner Schichten und zur Mikrowägung," *Zeitschrift für Physik* **155**, 206 (1959).
⁵⁶H. P. Koidl, W. F. Rieder, and Q. R. Salzmann, *IEEE Trans. Compon., Packag. Manuf. Technol.* **22**, 439 (1999).
⁵⁷H. P. Koidl, W. F. Rieder, and Q. R. Salzmann, *IEEE Trans. Compon., Packag. Manuf. Technol.* **23**, 222 (2000).
⁵⁸R. C. Weast and M. J. Astle, *CRC Handbook of Chemistry and Physics*, CRC Press, Boca Raton, FL (1980).
⁵⁹F. Kruchten, K. Knorr, U. G. Volkmann, H. Taub, F. Y. Hansen, B. Matthies, and K. W. Herwig, *Langmuir* **21**, 7507 (2005).
⁶⁰MATERIAL SAFETY DATA SHEET n-Dodecane. Version 1.2, MSDS Number:100000014121 (2010).
⁶¹P. V. Schwartz, D. J. Lavrich, and G. Scoles, *Langmuir* **19**, 4969 (2003).
⁶²B. Jensen, L. Chow, K. Huang, K. Saitou, J. Volakis, and K. Kurabayashi, *J. Microelectromech. Syst.* **14**, 935 (2005).
⁶³D. J. Wold and C. D. Frisbie, *J. Am. Chem. Soc.* **123**, 5549 (2001).
⁶⁴M. Paulsson, F. Zahidy, and S. Datta, *Nanoscience, Engineering and Technology Handbook*, (CRC Press, Boca Raton, FL, 2002).